DOI: 10.1002/ejic.200900399

On the Chemistry of the Strong Organic Electron-Donor 1,2,4,5-Tetrakis(tetramethylguanidino)benzene: Electron Transfer in Donor–Acceptor Couples and Binuclear Late Transition Metal Complexes

Anastasia Peters,[a] Christine Trumm,[a] Matthias Reinmuth,[a] Dimitri Emeljanenko,[a] Elisabeth Kaifer,[a] and Hans-Jörg Himmel*[a]

Keywords: Redox chemistry / N ligands / Electron transfer / Donor–acceptor systems

In this work we report on some aspects of the chemistry of the organic electron-donor 1,2,4,5-tetrakis(tetramethylguanidino)benzene (ttmgb). Reactions with electron acceptors and proton donors as well as late transition metals to give binuclear complexes (including a binuclear Cu^{II} complex with antiferromagnetic coupling through the bridging ttmgb ligand) are analysed. These studies shed some light on the electron-donor/proton-acceptor and coordination behaviour of this compound.

Introduction

Organic molecular electron donors and acceptors are of interest for the synthesis of new organic conductors or superconductors,[1] as mild reagents for redox reactions[2] and also as "noninnocent" complex ligands.[3] Recently, we reported on the syntheses of a new strong molecular electron donor, namely, 1,2,4,5-tetrakis(tetramethylguanidino)benzene [ttmgb; see Equation (1)].[4] Oxidation of ttmgb occurs slowly with O_2 from the air and spectroscopic data indicate two-electron oxidation. Reaction with the electron acceptor I_2 leads to oxidation of the tetraguanidine to give $[ttmgb](I_3)_2$ [Equation (1)]. Variations in the C–C bond lengths within the C_6 ring indicate loss of aromaticity upon oxidation. In this work we discuss now in detail the chemical properties of ttmgb.

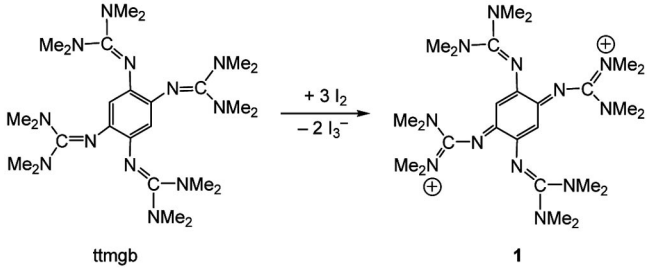

ttmgb **1** (1)

[a] Anorganisch-Chemisches Institut, Ruprecht-Karls-Universität Heidelberg,
Im Neuenheimer Feld 270, 69120 Heidelberg, Germany
Fax: +49-6221-545707
E-mail: hans-jorg.himmel@aci.uni-heidelberg.de

Supporting information for this article is available on the WWW under http://dx.doi.org/10.1002/ejic.200900399.

Results and Discussion

In the following we report in turn on the results obtained with an electron acceptor and proton donor and with some late-transition-metal salts of group 12, 11 and 10 (Zn^{II}, Cu^{II} and Pt^{II}), leading to binuclear complexes of neutral or oxidised ttmgb.

Electron- and Proton-Transfer Reactions with Acceptor Molecules

As mentioned in the Introduction, we already reported on the two-electron oxidation of ttmgb with I_2.[4] Purple-black-coloured crystals of a metal-like appearance were obtained from the reaction mixture, which turned out to be composed of $[ttmgb][I_3]_2$ (**1**). When these crystals were dissolved in dmso, a fast reaction occurred, and the isolated reaction product turned out to be $[C_6I_2\{NC(NMe_2)_2\}_4][I_3]_2$ (**2**). Thus, the two C–H bonds in the C_6 ring of $[ttmgb]^{2+}$ were replaced by C–I bonds. One possible explanation for this reaction includes the I_2-catalysed disproportionation of dmso [Equation (2)].[5] As a result of the high dielectric constant of dmso, the 1:1 complex between $(CH_3)_2S$ and I_2 ionises into $(CH_3)_2SI^+$ and I^-.[5] Aryl halogenation using $(CH_3)_2SI^+$ then leads to product **2**. Three equivalents of **1** can be transformed into two equivalents of **2** (leading to a maximum possible yield of 67%). With 59%, the experimentally obtained yield is slightly lower. The molecular structure as derived from X-ray diffraction is visualised in Figure 1. Figure 2 illustrates the packing of the ions in the crystal in quasi-1D rows. The figure also shows a photo of the crystalline material. Like **1**, solid **2** has a metal-like appearance. Conduction measurements for **1** as well as for **2** are on the

way.[6] As anticipated, the structure of the $[C_6I_2\{NC(NMe_2)_2\}_4]^{2+}$ dication resembles that of $[ttmgb]^{2+}$ in $[ttmgb][I_3]_2$. Thus, the C–C distances within the C_6 ring vary significantly, the shortest being 137.6(7) pm (C2–C3′) and the largest being 150.6(7) pm (C1–C2), indicating the absence of aromaticity. The short C1–N1 bond length of 129.6(7) pm suggests double-bond character and the larger C2–N4 bond length of 134.7(6) pm suggests single-bond character. The replacement of the two C–H by C–I bonds should bring about increased reactivity and might especially open up a way to link two or more of the electron donor units or donor–acceptor units together. Experiments to replace the iodine atom by alkynes or NH_2 [and then $NC(NMe_2)_2$] are currently under way.

$$(CH_3)_2SO \bullet I_2 \rightleftharpoons (CH_3)_2SO_2 + (CH_3)_2S \bullet I_2$$
$$(CH_3)_2S \bullet I_2 \rightleftharpoons (CH_3)_2SI^+ + I^- \quad (2)$$

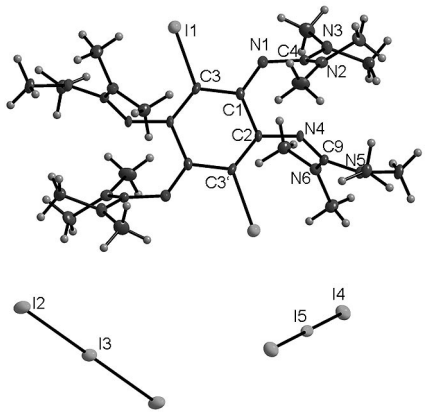

Figure 1. Molecular structure of the dication in $[C_6I_2\{NC(NMe_2)_2\}_4][I_3]_2$ (**2**). Thermal ellipsoids are drawn at the 50% probability level.

In subsequent reactions we probed the redox chemistry with another electron acceptor, namely, chloranilic acid, which will be denoted H_2ca in the following. This molecule is an electron acceptor as well as a proton donor. Our experiments show that in this case, proton-transfer reactions are favoured over redox reactions and result in the formation of the salt $[ttmgbH_4][ca]_2{\cdot}6H_2O$ (**3**). Figure 3 illustrates the structure of one $[ttmgbH_4]^{4+}$ cation together with its two adjacent $[ca]^{2-}$ units and two water molecules, which all are connected through hydrogen bonding. Figure 4 sketches the packing of the donor and the acceptor units in the crystal. Interestingly, the electron-donor units are arranged in stacks. As a result of the bulky *N*-methyl groups pointing upwards and downwards, the interplanar distance between the aromatic rings of two neighbouring molecules within the stack is unfortunately too large to allow stronger intermolecular π···π interactions. The bond lengths C14–19, C17–C18 and C18–C19 measure 139.42(19), 140.13 and 154.74(18) pm, respectively. For comparison, in the salt $[ImH]_2[ca]$ (Im = imidazole), the C–C bond lengths are 136.5(3), 141.0(3) and 154.0(3) pm, respectively.[7] In neutral $H_2ca{\cdot}2H_2O$, C–C bond lengths of 151.2, 134.5 and

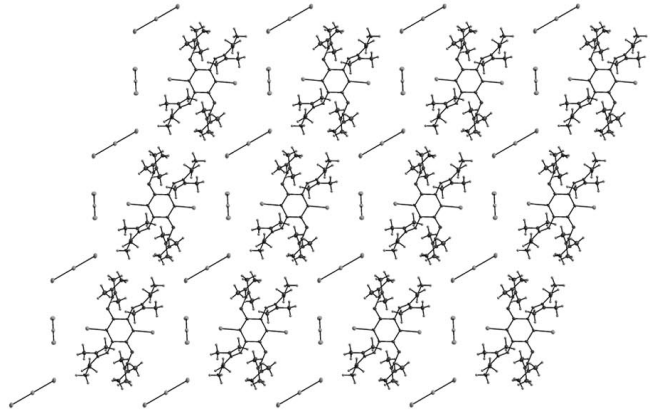

Figure 2. Illustration of the packing of the $[C_6I_2\{NC(NMe_2)_2\}_4]^{2+}$ cations and I_3^- anions in crystals of $[C_6I_2\{NC(NMe_2)_2\}_4][I_3]_2$ (**2**). The figure also shows a photo of the obtained crystals.

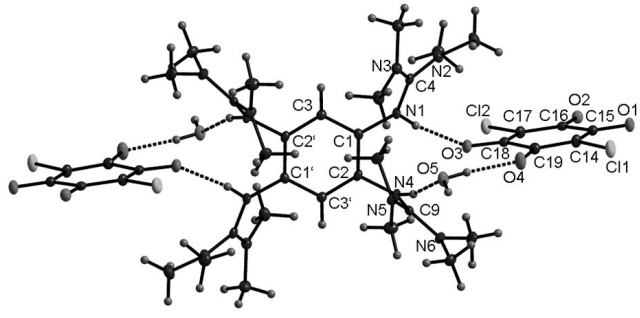

Figure 3. Molecular structure of the cations in $[ttmgbH_4][ca]_2{\cdot}6H_2O$ (**3**) showing coordination around one of the $[ttmgbH_4]^{4+}$ cations. Thermal ellipsoids are drawn at the 50% probability level.

144.6 pm were measured, which are in line with the presence of single and double bonds.[8] As anticipated, the C–C bond lengths shrink as a consequence of deprotonation.

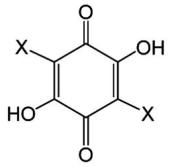

H_2ca: X = Cl

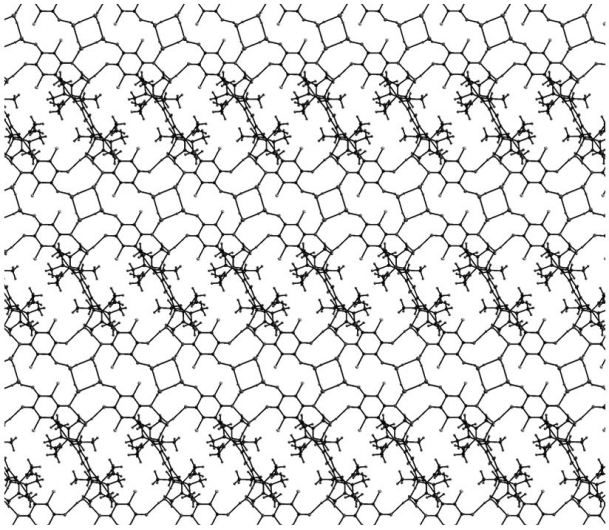

Figure 4. Illustration of the $[ttmgbH_4][ca]_2 \cdot 6H_2O$ network bound together through hydrogen bonding.

Binuclear Zn Complexes

We started our studies on late-transition-metal complexes of ttmgb with the reaction between ttmgb and $ZnCl_2$ in a 1:2 molar ratio. As anticipated, the product of this reaction turned out to be $[(Cl_2Zn)_2(ttmgb)]$ [**4**; Equation (3)]. The complex was crystallised from CH_3CN solution, and Figure 5 displays the molecular structure as derived from X-ray diffraction analysis. The unit cell contains two slightly different molecules (only one of these is shown in Figure 5). It can be seen that two imino N atoms of adjacent guanidino groups bind to the Zn atom, realising a κ^2-coordinational mode. The two Zn atoms are not located in the C_6 ring plane. Instead, the Zn atom is located ca. 16 pm (ca. 10 pm in the second molecule) below/above this plane, resulting in a "*trans*-type" conformation (see Figure 5). Both Zn atoms are coordinated in a distorted tetrahedral fashion. The N1–Zn–N4 bond angle is 82.87(9)°, whereas all other bond angles around the Zn atom fall into the range 113–117°. The Zn–N distances measure 203.8(2) pm. The small variations in the C–C distances within the C_6 ring (139.3, 140.6 pm) confirm the conservation of the aromatic system in the ttmgb ligand, which is thus not oxidised.

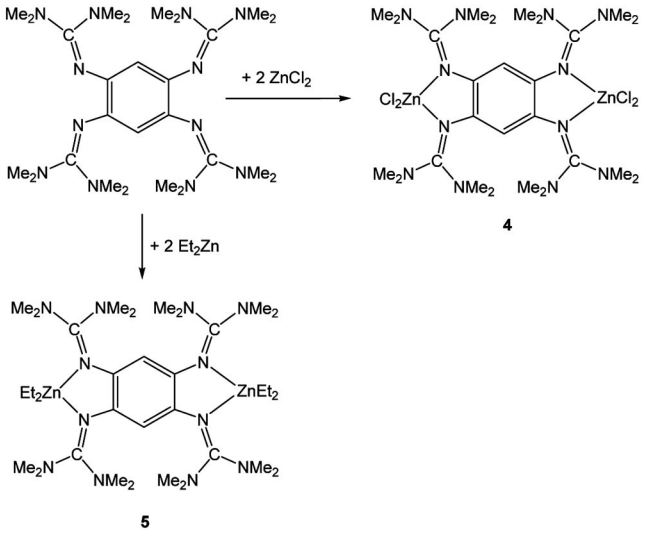

(3)

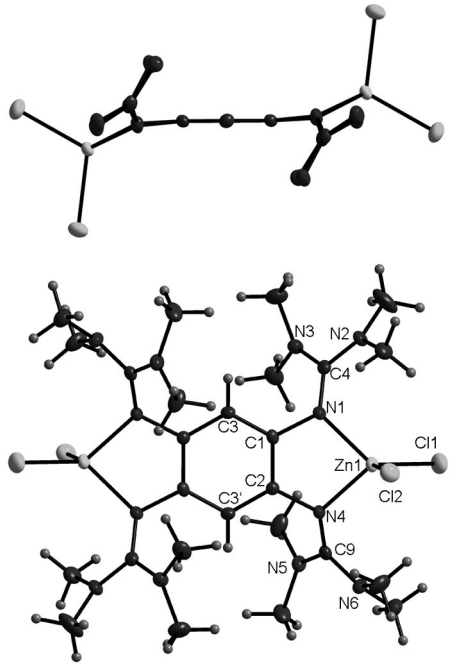

Figure 5. Molecular structure of $[(Cl_2Zn)_2(ttmgb)]$ (**4**). Thermal ellipsoids are drawn at the 50% probability level.

Furthermore, we synthesised the binuclear alkyl complex $[(Et_2Zn)_2(ttmgb)]$ (**5**) by reaction between ttmgb and Et_2Zn [Equation (3)]. In the ^1H NMR spectrum of CD_2Cl_2 solutions the ethyl ligands give rise to two quartets at $\delta = -0.33$ and –0.46 ppm due to the CH_3 groups and a multiplet at $\delta = 0.95$ ppm due to the CH_2 protons. The two protons of the benzene ring appear at $\delta = 5.39$ ppm. A broad multiplet in the region $\delta = 2.1$–3.1 ppm can be assigned to the guanidino methyl groups. Rapid fluctuations within the guanidino groups (rotations around the C–N bond axis, inversions at the N atoms) can be responsible for the equivalence of

the methyl groups on the NMR timescale. It has been shown previously for complexes of bis(tetramethylguanidino)benzene (btmgb) that lower temperatures are necessary to freeze these fluctuations.[9] The IR spectrum shows a very strong absorption with its maximum at 1549 cm^{-1} in a region characteristic of the ttmgb ligand, which can be assigned to vibrational modes with some character from the stretch ν(C=N). Figure 6 visualises the molecular structure of **5**. Selected structural details from our X-ray diffraction analysis are included in Table S4 (Supporting Information). Again, the Zn atoms are dislocated from the plane defined by the aromatic ring, resulting in a chair-type conformation with the Zn atoms being located on opposite sides of this plane. The higher electron density at the Zn atoms in **5** compared with **4** leads to larger Zn–N distances [219.97(19) and 223.22(19) pm, elongated by more than 16 pm with respect to **4**]. The chemical properties (e.g., with respect to alkylation) of this new, relatively stable Zn alkyl complex are currently under investigation. Interestingly, alkylation of the N=C bonds within the guanidino groups does not take place, even at elevated temperatures. In this respect, complex **4** behaves similarly to mononuclear alkyl complexes of bisguanidino ligands.[9]

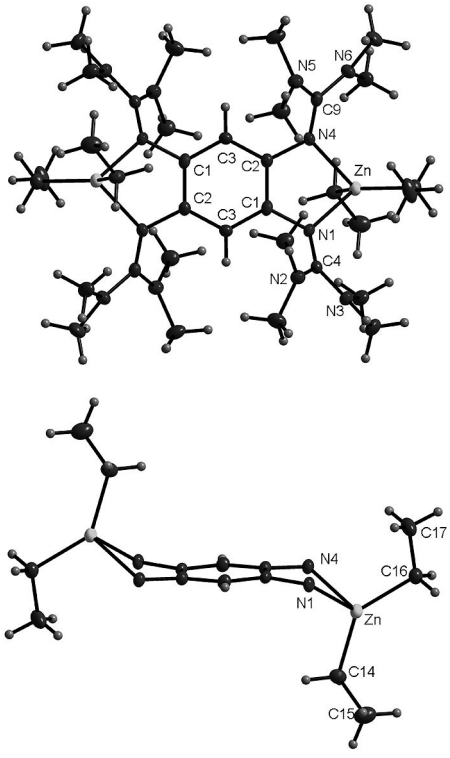

Figure 6. Molecular structure of $[(Et_2Zn)_2(ttmgb)]$ (**5**). Thermal ellipsoids are drawn at the 50% probability level.

Binuclear Cu^{II} Complex

Next, the donor ttmgb was treated with an excess amount of the Cu^{II} salt $Cu(BF_4)_2{\cdot}xH_2O$ (x = 5.5 according to elemental analysis). Reaction in CH_3CN yielded dark-green-coloured crystals. At the same time, the inner glass surface of the reaction vessel got coated with a Cu metal film, indicating reduction of the Cu^{II} ions.[10] In the mass spectrum (FAB) of the product, a strong signal appeared at m/z = 657.4, which can be assigned to $[Cu_2(ttmgb)]^+$. Thus, the mass spectrum is in line with the formation of a binuclear Cu complex. The IR spectrum contained strong absorptions around 1616 cm^{-1}, arguing for the presence of the ttmgb ligand in the product. No signals of the reaction product were visible in the ^1H NMR spectrum, signalling the formation of a paramagnetic Cu^{II} complex. The UV/Vis spectrum (see Supporting Information) of CH_3CN solutions displayed three bands with absorption maxima at λ = 212, 280 and 416 nm. A sharp peak in the CV curve recorded for the product dissolved in CH_3CN appears at $E_{1/2}$ = –1.13 V (Pt electrodes) and can be assigned to the Cu^{II}/Cu^{I} couple {see for comparison the CV curves measured recently for mononuclear (guanidino)Cu^{I} complexes[11]}. Thus, all spectroscopic experiments point to the formation of a binuclear Cu^{II} complex of the oxidised ttmgb ligand. The molecular structure of the complex was finally analysed by single-crystal X-ray diffraction. Large block-shaped crystals were grown directly from the condensed reaction mixture (CH_3CN solution). Figure 7 displays one of the crystals with an edge length of more than 2 mm. From the XRD analysis the product can be identified unambiguously as the salt $[\{(CH_3CN)_4Cu\}_2(ttmgb)][BF_4]_6$ (**6**). Thus, the reaction proceeds according to Equation (4). The crystal contains cocrystallised CH_3CN molecules in a fourfold excess. Figure 7 sketches the molecular structure of one cationic unit as derived from X-ray diffraction. Selected structural parameters can be found in Table S5 (Supporting Information). The formal oxidation state of the coordinating Cu atoms in this unit is +II, and the ligand is formally oxidised to $[ttmgb]^{2+}$. The Cu^{II} atoms are coordinated in a highly distorted (elongated) octahedral fashion (4+1+1 coordination). The Cu–N distances to the axial CH_3CN ligands [232.12(14) and 283.0(2) pm] are much larger than the equatorial ones [198.62(14) and 198.80(17) pm]. With 199.85(14) and 199.84(16) pm, the Cu–N distances to the ttmgb ligand units are within the accuracy of the measurement identical and similar to the distances to the equatorial CH_3CN ligands. The variations in the C–C bond lengths within the central C_6 ring confirm oxidation of the ttmgb ligand. Thus, the C1–C2 bond length amounts to 150.21(19) pm and can be considered as a single bond, whereas a distance of 138.8(2) pm of the C2–C3 bond length is in line with a double bond {see also the similar values [136.3(4) pm and 149.1(4) pm] derived for **1**}.[4]

The complex was further analysed by magnetic (SQUID) measurements. In Figure 8a the magnetic susceptibility χ_M is plotted in dependence of the temperature for a polycrystalline powder sample of **6**. The form of the curve indicates antiferromagnetic coupling. It can be fitted with the standard formula for the temperature dependence of the molar magnetic susceptibility in dinuclear Cu^{II} complexes, where N_A, β and k represent the Avogadro number, the Bohr magneton and the Boltzmann constant, respectively; the fit pa-

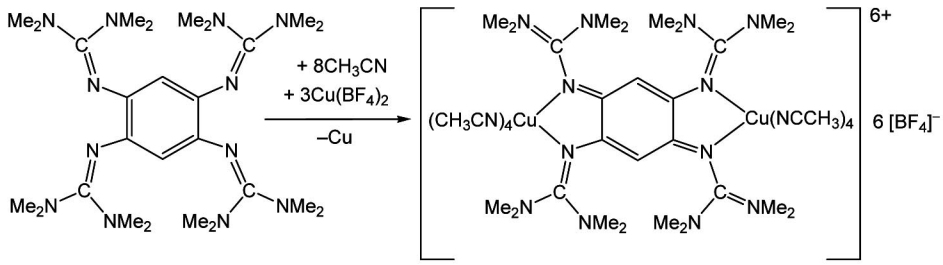

6 (4)

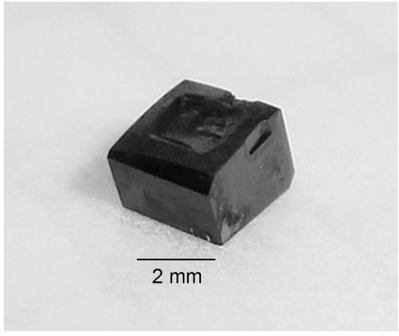

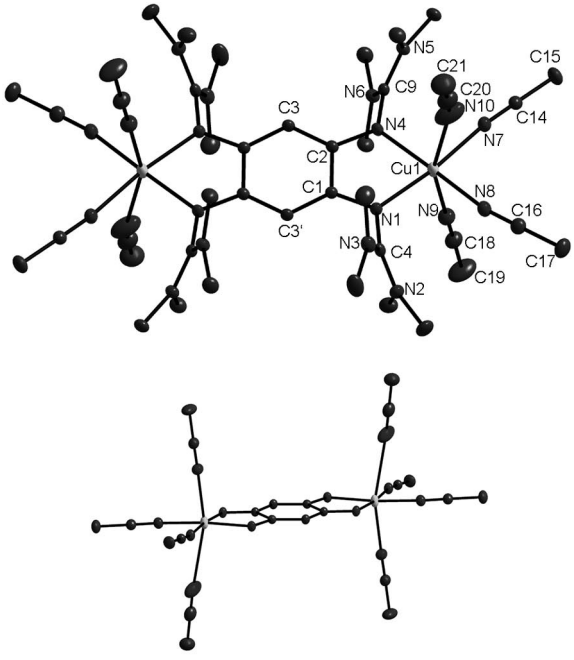

Figure 7. Molecular structure of the cation in $[\{(MeCN)_4Cu\}_2(ttmgb)][BF_4]_6 \cdot 4MeCN$ (**6**). Thermal ellipsoids are drawn at the 50% probability level. The figure also shows a photo of one of the obtained crystals.

rameters are the Zeeman factor g_{mag}, the proportion of noncoupled paramagnetic impurities (the molecular weight of which was assumed to be equal to that of the binuclear complex) expressed by ρ, and the S–T energy gap J.

$$\chi_M = \frac{2N\beta^2 g_{mag}^2}{kT}\left[3+\exp\left(\frac{-J}{kT}\right)\right]^{-1}(1-\rho)+\frac{N\beta^2 g_{mag}^2}{2kT}\rho$$

Figure 8 displays the curve resulting from a fit with g_{mag} = 2.02 (slightly above the free electron value), ρ = 0.017 and J = –35.4 cm^{-1}. The negative sign of J confirms the presence of antiferromagnetic coupling. The magnitude of J shows that the interaction of the two magnetic orbitals is not strong, but still significant. It is very similar, for example, to that observed recently for binuclear complexes with a bridging ca (deprotonated chloranilic acid) ligand.[12] With 790.2 pm, the Cu···Cu separation in **6** is too large for significant direct dipole–dipole interaction. From Figure 7 one can see that the copper basal planes and the ligand plane (note that the C_6 ring is not completely planar) are almost coplanar. The relative orientation of the magnetic orbitals thus could allow significant magnetic coupling[13] despite the large Cu···Cu separation. Figure 8b displays an EPR spectrum at X-band frequency measured for polycrystalline

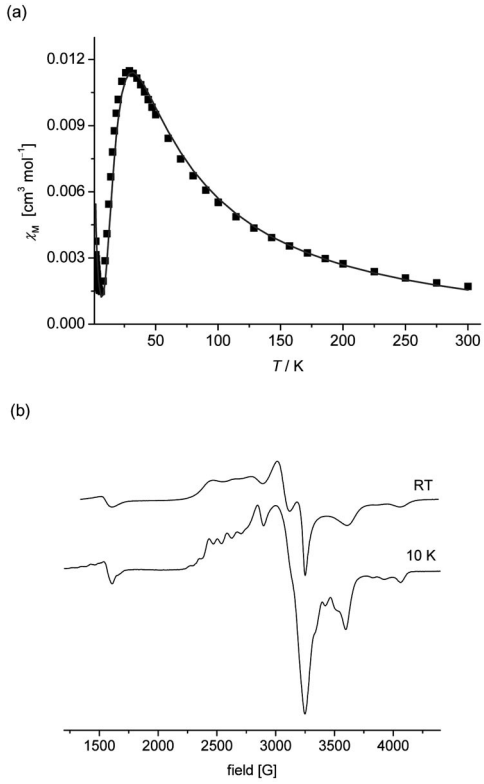

Figure 8. (a) SQUID magnetic curve for polycrystalline powder material of **6**; (b) polycrystalline powder EPR spectrum (295 K) of **6** at X-band frequency (B_0 = 3368 G).

powder material of **6** at room temperature. Most importantly, the spectrum features, in addition to signals from transitions $\Delta M_s = \pm 1$, a signal due to the half-field transition at 1557 G in line with the presence of magnetic coupling between the two Cu^{II} ions. Detailed analysis and estimation of the zero-field splitting parameters from the spectrum proved unfortunately to be difficult.[14] At low temperatures (ca. 10 K), hyperfine coupling becomes visible (see Figure 8b).

Binuclear Pt Complexes

Next we treated ttmgb with $Cl_2Pt(dmso)_2$ in CH_2Cl_2 solutions. The reaction proceeded to the complex [{(dmso)ClPt}$_2$(ttmgb)][$PtCl_3$(dmso)]$_2$ [**8**; see Equation (5)]. This binuclear complex exhibits two isomers with either a *cis*- or a *trans*-type conformation of the Cl and dmso ligands. As expected, the NMR spectra showed the presence of an equilibrium between the two isomers at room temperature and in solution. The relative concentrations of both isomers could easily be estimated from the ^{1}H signals of the aromatic protons. In the *trans* isomer, the two aromatic protons show at δ = 5.23 ppm, whereas in the *cis* isomer two signals appear at δ = 5.45 and 5.20 ppm. The relative molar ratio *trans*/*cis* amounts to ca. 2:1. In the ESI mass spectrum one could see, in addition to the intense peak of the dication, a weaker signal due to the monocation [{(dmso)ClPt}$_2$(ttmgb)][$PtCl_3$(dmso)]. The complex can be crystallised in its *trans*-isomeric form from CH_2Cl_2/hexane. Figure 9 displays the molecular structure as derived from X-ray diffraction. A structural comparison between this dinuclear complex (for a list of some structural parameters, see Table S6, Supporting Information) and the mononuclear complex obtained with the corresponding bisguanidine btmgb [1,2-bis(tetramethylguanidino)benzene][15] indicates that the ligand–metal bonding is similar. The dmso ligands in both complexes are bound through the S atom to the Pt. The Pt–N bond lengths of 204.1(6) and 201.8(5) pm in the dication [{(dmso)ClPt}$_2$(ttmgb)]$^{2+}$ compare with values of 203.6(3) and 201.5(3) pm in the monocation [(dmso)ClPt(btmgb)]$^+$. The N–Pt–N bond angles are also similar [79.3(2)° in the binuclear and 79.96(13)° in the mononuclear complex]. Finally, the donor properties of the ligands also seem to be comparable as indicated by the likeness of the imine N=C bond lengths {136.4(8) and 136.9(9) pm in [{(dmso)ClPt}$_2$(ttmgb)]$^{2+}$ and 135.6(5) and 137.5(5) pm in [(dmso)ClPt(btmgb)]$^+$}.

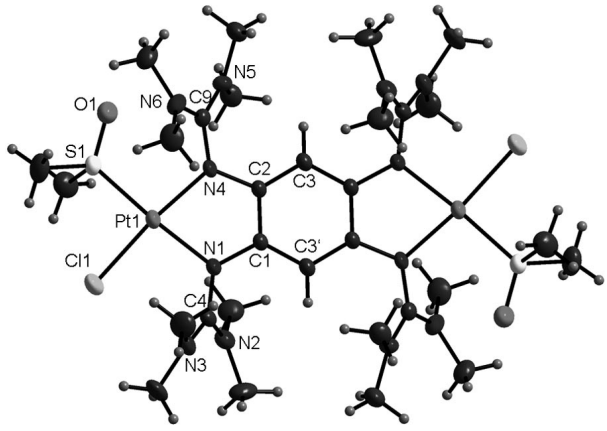

Figure 9. Molecular structure of the dication in [{(dmso)ClPt}$_2$(ttmgb)][$PtCl_3$(dmso)]$_2$ (**7**). Thermal ellipsoids are drawn at the 50% probability level.

When solutions of ttmgb in CH_3CN and $Cl_2Pt(dmso)_2$ in dmso were mixed, the reaction proceeded slightly differently to give the salt [{(dmso)ClPt}$_2$(ttmgb)]Cl_2. There are some reactivity differences between this complex and the related mononuclear complex [{(dmso)ClPt}(btmgb)]Cl. Hence, it was impossible to synthesise [{Cl_2Pt}$_2$(ttmgb)] simply by thermal treatment of [{(dmso)ClPt}$_2$(ttmgb)]Cl_2. Possibly a redox reaction takes place in the course of which the ligand is oxidised. An alternative route that was successfully applied to synthesise [Cl_2Pt(btmgn)] [btmgn, bis(tetramethylguanidino)naphthalene] was the reaction with Zeise's dimer [$PtCl_2(C_2H_4)$]$_2$.[16] Reaction between this dimer and btmgn gives first [$(C_2H_4)Cl_2Pt$(btmgn)], with a κ^1-coordinated btmgn ligand. This complex can subsequently be converted thermally in boiling CH_2Cl_2 solutions into [Cl_2Pt(btmgn)] (now with κ^2-coordination of the btmgn ligand).

The same route as applied in the [Cl_2Pt(btmgn)] synthesis was also applied in this work with the ttmgb ligand. Depending on the solvent (see Experimental Section), the isolated reaction product either is [{(C_2H_4)ClPt}$_2$(ttmgb)]-

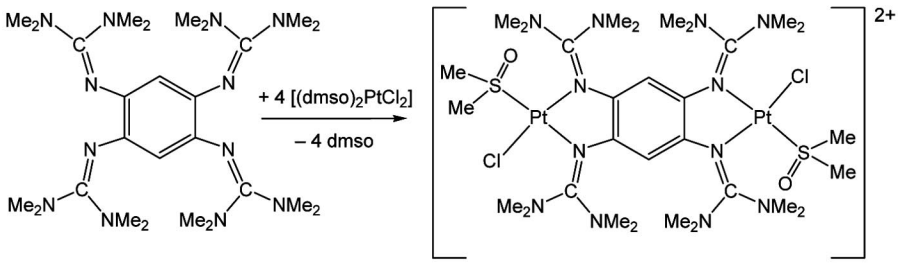

2 [$PtCl_3$(dmso)]$^-$

7 (5)

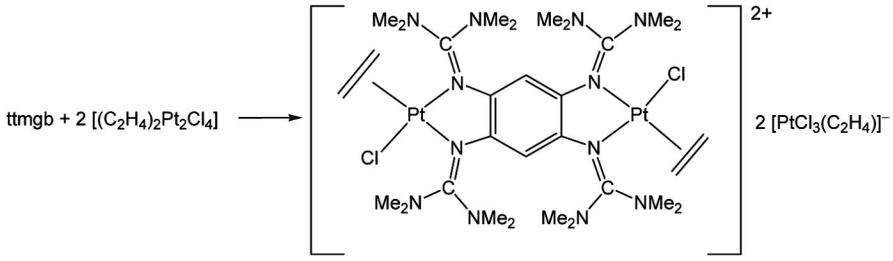

8 (6)

$[PtCl_3(C_2H_4)]_2$ (**8**), formed according to Equation (6) or $[\{(C_2H_4)ClPt\}_2(ttmgb)]Cl_2$. The ^1H NMR spectra again showed the presence of both the *trans* (signal at δ = 5.19 ppm) and *cis* (signals at δ = 5.31 and 5.11 ppm) isomer in solution at room temperature. The ratio *trans*/*cis* amounts to ca. 2.6 for **9**. In the IR spectrum of $[\{(C_2H_4)ClPt\}_2(ttmgb)]Cl_2$ weak bands at 1495 and 1469 cm^{-1} [being partially masked by larger absorptions from modes with contributions from the stretches ν(C=N)] can be assigned to ν(C=C) stretches, which are well known to be heavily coupled with the $\delta(CH_2)$ modes.[17] In the case of **8**, only one band at 1469 cm^{-1} was detected unambiguously [the other one(s) being visible as shoulder(s) near 1490 cm^{-1}, but not well resolved]. For comparison, the corresponding mode in free C_2H_4 occurs at 1623 cm^{-1}. The redshift can be explained classically by back donation of electron density from an occupied metal orbital into antibonding π* orbitals at the C_2H_4 ligand. Crystals of **8** in its *trans* form suitable for X-ray diffraction could be grown from CH_3CN solutions layered with toluene. Figure 10 displays the structure of one of the $[\{(C_2H_4)ClPt\}_2(ttmgb)]^{2+}$ units (Table S7, Supporting Information). The ttmgb ligand is κ^2-coordinated to each Pt atom and the Pt–N distances measure 201.0(5) and 202.3(0) pm. With 129.3(10) pm, the value determined by X-ray diffraction for the C=C bond in the ethylene unit is certainly too small.[18] The C=C bond length in free ethylene amounts to 133.7(2) pm,[19] and coordination is not expected to lead to a decrease in this value (see also the IR data). From Figure 10 it can be seen that one of the ellipsoids (at C14) is much larger than the other one, and this relatively large vibrational amplitude could lead to an underestimation of the C=C bond length. In this respect, complex **8** is of course no isolated example. Thus, standard X-ray diffraction analysis found for the cationic complex $[Ag(\eta^2\text{-}C_2H_4)_3]^+$ an average C=C bond length of 130.4 pm, which only very slightly increases (to 130.7 pm) if additional standard corrections for vibration were made.[20] The Pt–C distances in the cationic part of **8** came out to be 212.9(6) (Pt–C14) and 214.7(6) pm (Pt–C15) and are on average slightly larger than the Pt–C distances in $[(C_2H_4)Cl_2Pt(btmgn)]$ [211.9(6) and 213.8(7) pm]. The Pt–N bond lengths measure 201.0(5) and 202.3(0) pm. Complex **8** is interesting for catalytic applications. We already showed that Pt complexes featuring bisguanidino ligands can be active catalysts in hydrosilylation reactions.[16] Hence, $[Cl_2Pt(btmgn)]$ was found to be inactive as a catalyst in hydrosilylation, but $[(C_2H_4)Cl_2Pt(btmgn)]$ turned out to be highly active. In addition to its catalytic properties, we are especially interested in using the olefin complex to align the strong electron-donor molecule ttmgb into polymeric chains. This aim can be achieved by replacing the C_2H_4 ligand by dienes such as norbornadiene, linking the complexes together.[21]

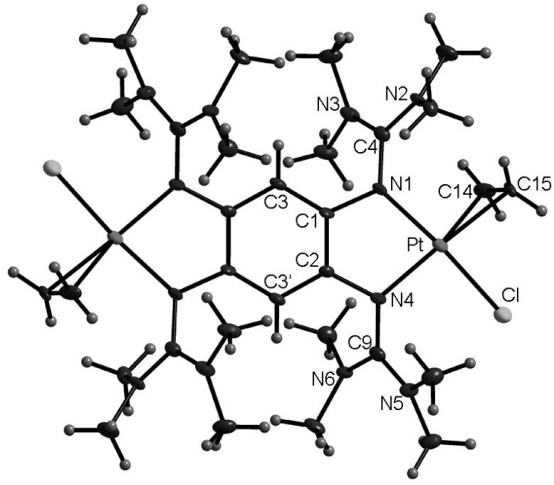

Figure 10. Molecular structure of the dication in $[\{(C_2H_4)ClPt\}_2(ttmgb)][PtCl_3(C_2H_4)]_2$ (**8**). Thermal ellipsoids are drawn at the 50% probability level.

Conclusions

In this work we first analysed the donor capacity and proton-acceptor properties of the newly synthesised tetraguanidino compound 1,2,4,5-tetrakis(tetramethylguanidino)benzene (ttmgb). Reaction with I_2 leads to a redox reaction to $(ttmgb)(I_3)_2$. Interestingly, aryl halogenation yielding the $[C_6I_2(NCNMe_2)_4]^{2+}$ dication is observed when this compound is dissolved in dmso. The isolated salt $[C_6I_2(NCNMe_2)_4](I_3)_2$ exhibits a metal-like appearance. The unexpected functionalisation of the ttmgb molecule opens up the possibility to link several donor units or donor–acceptor pairs together. In additional experiments we treated ttmgb with the electron-acceptor and proton-donor chloranilic acid (H_2ca) and obtained $[ttmgbH_2](ca)_2$ as

product. Thus, protonation is favoured over the redox reaction. Subsequently, we reported on the synthesis and characterisation of the first binuclear complexes of the ttmgb ligand. The examples discussed herein include a Cu^{II} complex with antiferromagnetic coupling between the two unpaired electrons mediated through the (oxidised) bridging ttmgb ligand. The experiments show that ttmgb is a good chelating redox-active ligand for the synthesis of binuclear transition-metal complexes. In future studies we seek to build metal-free and metal-containing oligomeric or polymeric chains containing the redox-active ttmgb ligand and to further explore magnetic exchange through the bridging ttmgb ligand in binuclear magnetic complexes.

Experimental Section

General: All reactions were carried out under a purified argon atmosphere and by using standard Schlenk techniques. Chloranilic acid (caH_2) and $Cu(BF_4)_2{\cdot}xH_2O$ ($x \approx 5.5$ according to elemental analysis) were purchased from Aldrich. The two Pt^{II} starting compounds $K_2[PtCl_4]$ (purity 99.9%) and $[PtCl(C_2H_4)(\mu\text{-}Cl)]_2$ (purity 97%) were obtained from ABCR and used as delivered. $Pt(dmso)_2Cl_2$ was prepared according to the literature.[22] The synthesis of the btmgb ligand and the $[btmgb](I_3)_2$ salt were described previously.[4] NMR spectra were measured with a Bruker Avance II 400 spectrometer at a temperature of 23 °C and referenced to known standards, and IR spectra were recorded with a Bruker Vertex 80v spectrometer. A Perkin–Elmer Lambda 19 spectrometer was used for UV/Vis spectroscopy.

$[C_6I_2\{NC(NMe_2)_2\}_4][I_3]_2$ (2): A solution of $[ttmgb][I_3]_2$ (0.211 g, 0.16 mmol) in dmso (10 mL) was heated to 100 °C for a period of 30 min. Then, dmso was removed in vacuo, and the residue was recrystallised from CH_3CN to yield **2** (0.146 g, 0.095 mmol, 59%). $C_{26}H_{48}I_8N_{12}$ (1543.96): calcd. C 20.23, H 3.13, N 10.89; found: C 21.39, H 3.49, N 11.46. ^1H NMR (600.13 MHz, [D$_6$]dmso): δ = 2.86 (s, 48 H, CH_3) ppm. $^{13}C\{^1H\}$ NMR (100.56 MHz, [D$_6$]dmso): δ = 164.08, 164.05, 164.02, 154.05, 78.30, 39.90 (CH_3) ppm. IR (CsI): $\tilde{\nu}$ = 2951 (w), 1615 (s), 1587 (s), 1499 (vs), 1465 (vs), 1416 (vs), 1397 (vs), 1280 (s), 1248 (s), 1177 (s), 1157 (s), 1041 (m), 1020 (s), 898 (m), 825 (m), 770 (w), 748 (s), 715 (m), 677 (w), 637 (m), 593 (m), 564 (w) cm^{-1}. UV/Vis (CH_3CN, $c = 1.23 \times 10^{-5}$ M): λ (ε, $M^{-1}cm^{-1}$) = 288 (10.84×10^4), 365 (4.86×10^4) nm. MS (FAB): *m/z* (%) = 783 (100) $[M]^+$, 738 (36) [**2** – HN$(CH_3)_2$], 657 (49) [**2** – I], 612 (16) [**2** – HN$(CH_3)_2$ – I]. Crystal data for $C_{26}H_{48}I_8N_{12}$: M_r = 3087.92, $0.30 \times 0.25 \times 0.25$ mm^3, triclinic, space group $P\bar{1}$, a = 10.055(2) Å, b = 10.113(2) Å, c = 12.300(3) Å, α = 96.28(3)°, β = 99.32(3)°, γ = 112.61(3)°, V = 1119.0(4) Å^3, Z = 1, $d_{calcd.}$ = 2.291 Mg m^{-3}, Mo-K_α radiation (graphite monochromated, λ = 0.71073 Å), T = 200 K, θ_{range} 1.71 to 33.78°. Reflections measured 28369, independent 8928, R_{int} = 0.0443. Final R indices [$I > 2\sigma(I)$]: R_1 = 0.0473, wR_2 = 0.1286.

$[ttmgbH_4][ca]_2$ (3): A solution of H_2ca (chloranilic acid; 0.058 g, 0.28 mmol) in CH_3CN (20 mL) was added to a solution of ttmgb (0.0744 g, 0.14 mmol) in CH_3CN (20 mL). Compound **3** precipitated from the reaction mixture in the form of a red-coloured solid. The solid was washed with CH_3CN and dried in vacuo. Product **3** (0.11 g, 0.12 mmol, 79%) was obtained, which can be recrystallised from H_2O or CH_3CN. ^1H NMR (399.89 MHz, D_2O): δ = 6.25 (s, 2 H), 2.80 (s, 48 H, CH_3) ppm. $^{13}C\{^1H\}$ NMR (100.56 MHz, D_2O): δ = 173.60, 106.21 (CH), 39.56 (CH_3) ppm. IR (CsI): $\tilde{\nu}$ = 2930 (w), 1635 (vs), 1542 (vs), 1516 (vs), 1416 (s), 1310 (m), 1245 (w), 1168 (m), 1068 (m), 1038 (m), 906 (m), 825 (s), 779 (w), 712 (w), 573 (m) cm^{-1}. MS (FAB): *m/z* (%) = 531 (100) $[(ttmgb)(H)]^+$, 486 (41) [ttmgb – N$(CH_3)_2$], 460 (13) [ttmgb – N$(CH_3)_2$CN], 414 (8) [ttmgb – NCN$(CH_3)_2$], 386 (16), 343 (14). Crystal data for **3**·$6H_2O$: M_r = 1056.82, $0.20 \times 0.25 \times 0.15$ mm^3, monoclinic, space group $P\bar{1}$, a = 9.3520(19) Å, b = 19.686(4) Å, c = 13.426(3) Å, β = 94.68(3)°, V = 1119.0(4) Å^3, Z = 2, $d_{calcd.}$ = 1.425 Mg m^{-3}, Mo-K_α radiation (graphite-monochromated, λ = 0.71073 Å), T = 100 K, θ_{range} 1.84 to 27.52°. Reflections measured 41077, independent 5653, R_{int} = 0.0472. Final R indices [$I > 2\sigma(I)$]: R_1 = 0.0322, wR_2 = 0.0834.

$[(ZnCl_2)_2(ttmgb)]$ (4): $ZnCl_2$ (1 M in Et_2O, 0.7 mL) was added dropwise to a solution of ttmgb (0.2046 g, 0.3854 mmol) in CH_3CN (20 mL). Subsequently, the reaction mixture was stirred at room temperature for 20 h. The solvent was removed in vacuo, and the residue washed with toluene (3×8 mL) to remove trace amounts of unreacted ttmgb. After removal of all solvent molecules in vacuo, **4** was obtained (0.2849 g, 0.3546 mmol, 92%) in the form of a colourless powder. The product was recyrstallised from CH_3CN at –21 °C. $C_{26}H_{50}Cl_4N_{12}Zn_2$ (803.36): calcd. C 38.87, H 6.27, N 20.92; found C 38.49, H 6.28, N 20.20. ^1H NMR (400 MHz, CD_2Cl_2): δ = 5.62 (s, 2 H), 2.87 (br. s, 48 H) ppm. $^{13}C\{^1H\}$ NMR (100.55 MHz, CD_2Cl_2): δ = 164.36 (CN_3), 135.26 (arom. C), 110.19 (arom. CH), 40.52 (NCH_3) ppm. IR (KBr): $\tilde{\nu}$ = 2999 (w), 2928 (m), 2883 (m), 2799 (w), 1547 (vs) 1481 (s), 1397 (s), 1333 (m), 1260 (m), 1232 (m), 1180 (m), 1153 (m), 1061 (w), 1029 (m), 959 (w), 892 (m), 868 (m), 810 (w), 719 (m), 660 (w), 580 (w), 410 (w) cm^{-1}. CV (CH_2Cl_2, vs. SCE): +0.33 V. HRMS (FAB+): calcd. for $C_{26}H_{50}N_{12}Cl_4Zn_2$ $[M]^+$ 802.1641; found 802.1608. MS (FAB+): *m/z* = 802.2 $[M]^+$, 767.3 $[M - Cl]^+$, 666.4 $[(ttmgb)ZnCl_2]^+$, 629.4 $[(ttmgb)ZnCl]^+$, 530.5 $[ttmgb]^+$. Crystal data for **4**·2MeCN: M_r = 885.42, $0.30 \times 0.25 \times 0.20$ mm^3, triclinic, space group $P\bar{1}$, a = 12.198(2) Å, b = 13.859(3) Å, c = 15.075(3) Å, α = 95.97(3)°, β = 108.39(3)°, γ = 109.63(3)°, V = 2213.9(8) Å^3, Z = 2, $d_{calcd.}$ = 1.328 Mg m^{-3}, Mo-K_α radiation (graphite-monochromated, λ = 0.71073 Å), T = 200 K, θ_{range} 1.46 to 28.00°. Reflections measured 42782, independent 10584, R_{int} = 0.0641. Final R indices [$I > 2\sigma(I)$]: R_1 = 0.0471, wR_2 = 0.1118.

$[(Et_2Zn)_2(ttmgb)]$ (5): To a solution was of ttmgb (0.1191 g, 0.224 mmol) in thf (5 mL) was dropwise added Et_2Zn (1.5 M in toluene, 0.45 mL), and the reaction mixture was stirred at room temperature for 2 h. Layering of the solution with *n*-hexane (10 mL) und storage at –21 °C produced colourless crystals of $[(Et_2Zn)_2(ttmgb)]$. $C_{34}H_{70}N_{12}Zn_2$ (777.76): calcd. C 52.50, H 9.07, N 21.61, Zn 16.81; found C 52.28, H 9.04, N 21.09. ^1H NMR (400 MHz, CD_2Cl_2): δ = 5.39 (m, 2 H), 2.1–3.1 (m, 48 H), 0.95 (m, 12 H), –0.33 (q, 4 H), –0.46 (q, 4 H) ppm. $^{13}C\{^1H\}$ NMR (100.55 MHz, CD_2Cl_2): δ = 160.94 (CN_3), 137.83 (arom. C), 111.95 (arom. CH), 39.44 (NCH_3), 14.78 (CH_3), 14.50 (CH_3), 3.71 (CH_2), 3.46 (CH_2) ppm. IR (KBr): $\tilde{\nu}$ = 2999 (w), 2924 (m), 2867 (m), 2822 (m), 2695 (w), 1549 (vs) 1479 (s), 1414 (s), 1386 (vs), 1267 (m), 1236 (m), 1178 (m), 1144 (s), 1063 (m), 1022 (s), 988 (m), 934 (m), 889 (w), 866 (m), 796 (w), 716 (m), 571 (m), 486 (m), 440 (m) cm^{-1}. Crystal data for **5**: M_r = 777.76, $0.20 \times 0.15 \times 0.15$ mm^3, monoclinic, space group $P2_1/c$, a = 9.927(2) Å, b = 13.259(3) Å, c = 15.650(3) Å, β = 90.24(3)°, V = 2059.9(7) Å^3, Z = 2, $d_{calcd.}$ = 1.254 Mg m^{-3}, Mo-K_α radiation (graphite-monochromated, λ = 0.71073 Å), T = 100 K, θ_{range} 2.01 to 31.00°. Reflections measured 13060, independent 6560, R_{int} = 0.0770. Final R indices [$I > 2\sigma(I)$]: R_1 = 0.0480, wR_2 = 0.1150.

$[\{(CH_3CN)_4Cu\}_2(ttmgb)][BF_4]_6$ (6): To a solution of ttmgb (214.5 mg, 0.40 mmol) dissolved at 70 °C in CH_3CN (25 mL) was added $Cu(BF_4)_2{\cdot}5.5H_2O$ (1020.5 mg, 3.04 mmol). The deep-green-

coloured reaction mixture was stirred for 30 min at 60 °C. Subsequently, the solution was slowly brought to room temperature, and the solvent was removed until 5 mL were left. After 24 h, **6** (303.7 mg, 50%) was obtained as deep-green-coloured crystals. IR (CsI): $\tilde{\nu}$ = 2931 (w), 1616 (m), 1500 (m), 1398 (s), 1310 (s), 1061 (vs), 1029 (vs), 893 (w), 520 (w) cm^{-1}. UV/Vis (CH_3CN, $c = 1.87 \times 10^{-5}$ M): λ (ε, $M^{-1}cm^{-1}$) = 212 (41027), 280 (11428), 416 (12888) nm. MS (FAB): *m/z* (%) = 657 (10) [Cu_2(ttmgb)], 530 (34) [ttmgb]$^+$, 460 (53) $[C_{16}H_{28}N_8Cu_2]^+$, 369 (64) $[C_{16}H_{28}N_6Cu]^+$. Crystal data for **6**·4MeCN: M_r = 1671.39, $0.40 \times 0.40 \times 0.30$ mm^3, triclinic, space group $P\bar{1}$, a = 12.385(3) Å, b = 12.811(3) Å, c = 14.464(3) Å, α = 86.19(3)°, β = 74.75(3)°, γ = 61.10(3)°, V = 1933.4(10) $Å^3$, Z = 1, $d_{calcd.}$ = 1.435 $Mg\,m^{-3}$, Mo-K_α radiation (graphite-monochromated, λ = 0.71073 Å), T = 100 K, θ_{range} 1.46 to 33.00°. Reflections measured 35260, independent 14592, R_{int} = 0.0340. Final R indices [$I > 2\sigma(I)$]: R_1 = 0.0450, wR_2 = 0.1197.

[{PtCl(dmso)}$_2$(ttmgb)]Cl$_2$: A solution of ttmgb (0.127 g, 0.24 mmol) in CH_3CN (20 mL) was added dropwise to a solution of $Pt(dmso)_2Cl_2$ (0.202 g, 0.48 mmol) in dmso (20 mL). The reaction mixture was stirred for 1 h at room temperature. Then, the solvent was removed in vacuo, and the remaining residue was redissolved in acetone. The product precipitated in the form of a red-coloured solid. $C_{30}H_{62}Cl_4N_{12}O_2Pt_2S_2$ (1219.01): calcd. C 29.56, H 5.13, N 13.78; found C 29.66, H 5.40, N 13.48. ^{1}H NMR (399.89 MHz, CD_3CN): δ = 5.31 [s, CH (*cis* isomer)], 5.23 (s, CH, *trans* isomer), 5.20 (s, CH, *cis* isomer), 3.35 [s, CH_3 (dmso)], 3.07 (s, CH_3), 3.05 (s, CH_3), 3.04 (s, CH_3), 3.02 (s, CH_3), 2.98 (s, CH_3), 2.96 (s, CH_3) ppm. $^{13}C\{^1H\}$ NMR (150.92 MHz, CH_3CN): δ = 166.58, 166.40, 164.80, 164.64, 138.13, 138.10, 138.05, 137.83, 99.52, 45.59, 42.24, 42.01, 41.75, 41.63, 41.28, 41.12, 40.41, 40.36 ppm. ^{195}Pt NMR (85.96 MHz, CH_3CN): δ = –2943.07, –2949.31 ppm. IR (CsI): $\tilde{\nu}$ = 2924 (w), 1596 (vs), 1515 (vs), 1487 (s), 1393 (vs), 1312 (s), 1239 (w), 1182 (m), 1137 (m), 1034 (m), 982 (m), 895 (m), 843 (w), 817 (w), 704 (w), 680 (w), 445 (w) cm^{-1}.

[{PtCl(dmso)}$_2$(ttmgb)][PtCl$_3$(dmso)]$_2$ (7): A solution of ttmgb (0.09 g, 0.17 mmol) in CH_2Cl_2 (10 mL) was dropwise added to a suspension of $Pt(dmso)_2Cl_2$ (0.158 g, 0.36 mmol) in CH_2Cl_2 (12 mL). Then, the reaction mixture was stirred for 1 h at room temperature. The solvent was removed in vacuo, and the remaining residue was redissolved in acetone. The product precipitated in the form of a red-coloured solid. After recrystallisation from CH_2Cl_2/hexane, deep-red coloured crystals were obtained. ^{1}H NMR (600.13 MHz, CD_3CN): δ = 5.31 (s, CH, *cis* isomer), 5.23 (s, CH, *trans* isomer), 5.20 (s, CH, *cis* isomer), 3.34 [s, CH_3 (dmso)], 3.27 {s, CH_3, dmso in ($[Pt(dmso)Cl_3]^-$)}, 3.07 (s, CH_3), 3.044 (s, CH_3), 3.035 (s, CH_3), 3.00 (s, CH_3), 2.98 (s, CH_3), 2.96 (s, CH_3) ppm. ^{13}C NMR (150.92 MHz, [D_6]dmso): δ = 166.58, 138.12, 138.10, 138.06, 99.52, 45.60, 43.89, 42.23, 42.01, 41.75, 41.63, 41.29, 41.13, 40.42, 40.37 ppm. IR (CsI): $\tilde{\nu}$ = 2917 (w), 1595 (vs), 1516 (vs), 1485 (s), 1466 (m), 1388 (vs), 1314 (s), 1289 (m), 1240 (w), 1187 (m), 1140 (s), 1119 (vs), 1022 (vs), 981 (m), 892 (m), 840 (w), 814 (w), 727 (w), 686 (w), 443 (m) cm^{-1}. MS (ESI): *m/z* (%) = 1527 (8) [(ttmgb)Pt_2Cl_2(dmso)$_2$][$PtCl_3$[dmso]]$^+$, 573 (100) [(ttmgb)Pt_2Cl_2(dmso)$_2$]$^{2+}$. Crystal data for $C_{34}H_{74}N_{12}Pt_4S_4$·$2.8CH_2Cl_2$: M_r = 4290.08, $0.30 \times 0.20 \times 0.15$ mm^3, triclinic, space group $P\bar{1}$, a = 12.668(3) Å, b = 12.866(3) Å, c = 13.662(3) Å, α = 101.86(3)°, β = 107.10(3)°, γ = 114.70(3)°, V = 1789.9(6) $Å^3$, Z = 1, $d_{calcd.}$ = 1.990 $Mg\,m^{-3}$, Mo-K_α radiation (graphite-monochromated, λ = 0.71073 Å), T = 200 K, θ_{range} 1.88 to 30.00°. Reflections measured 37769, independent 10416, R_{int} = 0.0560. Final R indices [$I > 2\sigma(I)$]: R_1 = 0.0507, wR_2 = 0.15431.

[{PtCl(C_2H_4)}$_2$(ttmgb)][PtCl$_3$(C_2H_4)]$_2$ (8): A solution of $Pt_2(C_2H_4)_2Cl_4$ (0.049 g, 0.043 mmol) in CH_3CN (6 mL) was added dropwise to a solution of ttmgb (0.022 g, 0.041 mmol) in CH_3CN (5 mL). The solvent was removed, and the remaining residue was redissolved in CH_3CN. Red-coloured crystals of **8** were obtained upon layering the solution with toluene. ^{1}H NMR (399.89 MHz, CD_3CN): δ = 5.31 (s, CH, *cis* isomer), 5.19 (s, CH, *trans* isomer), 5.11 (s, CH, *cis* isomer), 4.28 (s, CH_2, ethylene in $[PtCl_3(C_2H_4)]^-$), 3.95 (m, CH_2), 3.70 (m, CH_2), 3.12 (s, CH_3), 3.10 (s, CH_3), 2.96 (s, CH_3), 2.91 (s, CH_3) ppm. $^{13}C\{^1H\}$ NMR (100.56 MHz, CH_3CN): δ = 167.69, 165.10, 140.10, 139.25, 100.44, 67.90, 65.43, 41.85, 41.35, 41.00, 40.52 ppm. ^{195}Pt NMR (85.96 MHz, CH_3CN): δ = –2740.74, –3002.37 ppm. IR (CsI): $\tilde{\nu}$ = 2931 (w), 1597 (vs), 1513 (vs), 1467 (w), 1397 (vs), 1313 (vs), 1238 (w), 1185 (m), 1168 (m), 1037 (w), 983 (w), 891 (w), 847 (w), 817 (w), 709 (w), 502 (w), 468 (w) cm^{-1}. MS (ESI): *m/z* (%) = 1083 (76) [(ttmgb)$Pt_2Cl_2(C_2H_4)_2Cl]^+$, 524 (100) [(ttmgb)$Pt_2Cl_2(C_2H_4)_2]^{2+}$, 510 (25) [[(ttmgb)$Pt_2Cl_2(C_2H_4)_2$] – $C_2H_4]^{2+}$, 491 (89) [[(ttmgb)$Pt_2Cl_2(C_2H_4)_2$] – C_2H_4 – Cl]$^{2+}$. Crystal data for $C_{34}H_{66}N_{12}Pt_4$·$2CH_3CN$: M_r = 1789.02, $0.40 \times 0.20 \times 0.20$ mm^3, monoclinic, space group $P2_1/c$, a = 11.068(2) Å, b = 22.396(5) Å, c = 11.684(2) Å, β = 100.09(3)°, V = 2851.4(10) $Å^3$, Z = 2, $d_{calcd.}$ = 2.084 $Mg\,m^{-3}$, Mo-K_α radiation (graphite-monochromated, λ = 0.71073 Å), T = 100 K, θ_{range} 1.82 to 27.57°. Reflections measured 44343, independent 6546, R_{int} = 0.0657. Final R indices [$I > 2\sigma(I)$]: R_1 = 0.0364, wR_2 = 0.0745.

[{PtCl(C_2H_4)}$_2$(ttmgb)]Cl$_2$: A solution of $Pt_2(C_2H_4)_2Cl_4$ (0.028 g, 0.048 mmol) in CH_2Cl_2 (15 mL) was added dropwise to a solution of ttmgb (0.026 g, 0.048 mmol) in CH_2Cl_2 (10 mL). After stirring the solution at room temperature for 1 h the solvent was removed in vacuo. The product was redissolved in CH_3CN, and the product precipitated as a red-coloured solid upon the addition of toluene. $C_{30}H_{58}Cl_4N_{12}Pt_2$ (1118.84): calcd. C 32.21, H 5.22, N 15.02; found: C 32.10, H 5.30, N 14.64. ^{1}H NMR (600.13 MHz, CD_3CN): δ = 5.31 (s, CH, *cis* isomer), 5.21 (s, CH, *trans* isomer), 5.19 (s, CH, *cis* isomer), 3.82 (m, CH_2), 3.70 (m, CH_2), 3.13 (s, CH_3), 3.12 (s, CH_3), 3.11 (s, CH_3), 2.97 (s, CH_3), 2.96 (s, CH_3), 2.91 (s, CH_3), 2.91 (s, CH_3) ppm. $^{13}C\{^1H\}$ NMR (150.92 MHz, CH_3CN): δ = 167.71, 167.65, 165.09, 165.06, 140.08, 140.00, 139.49, 139.23, 101.39, 100.46, 99.83, 65.39, 65.37, 41.83, 41.82, 41.41, 41.33, 41.05, 40.97, 40.50, 40.49 ppm. ^{195}Pt NMR (85.96 MHz, CH_3CN): $\delta \approx$ –3005 (br. s) ppm. IR (CsI): $\tilde{\nu}$ = 2932 (w), 1597 (vs), 1506 (vs), 1500 (vs), 1495 (w), 1469 (w), 1397 (vs), 1313 (vs), 1235 (w), 1185 (m), 1167 (m), 1038 (w), 984 (w), 891 (w), 845 (w), 816 (w), 710 (w), 502 (w), 470 (w) cm^{-1}. MS (ESI): *m/z* (%) = 524 (100) [(ttmgb)Pt_2Cl_2-$(C_2H_4)_2]^{2+}$, 510 (95) [[(ttmgb)$Pt_2Cl_2(DMSO)_2$] – $C_2H_4]^{2+}$, 491 (87) [[(ttmgb)$Pt_2Cl_2(DMSO)_2$] – C_2H_4 – Cl]$^{2+}$.

X-ray Crystallographic Study: Suitable crystals were taken directly out of the mother liquor, immersed in perfluorinated polyether oil, and fixed on top of a glass capillary. Measurements were made with a Nonius-Kappa CCD diffractometer with a low-temperature unit by using graphite-monochromated Mo-K_α radiation. The temperature was set to 100 K. The data collected were processed by using the standard Nonius software.[23] All calculations were performed using the SHELXT-PLUS software package. Structures were solved by direct methods with the SHELXS-97 program and refined with the SHELXL-97 program.[24,25] Graphical handling of the structural data during solution and refinement was performed with XPMA.[26] Atomic coordinates and anisotropic thermal parameters of non-hydrogen atoms were refined by full-matrix least-squares calculations. CCDC-729245 (for **2**), -729246 (for **3**), -729247 (for **8**), -729248 (for **9**), -729249 (for **5**), -729250 (for **4**) and -729251 (for **6**) contain the supplementary crystallographic data for this paper. These data can be obtained free of charge from The Cambridge Crystallographic Data Centre via www.ccdc.cam.ac.uk/data_request/cif.

Supporting Information (see footnote on the first page of this article): Selected structural parameters from the XRD analysis of compounds **2**–**8**; spectroscopic data (UV/Vis, IR and CV) for complex **6**.

Acknowledgments

The authors gratefully acknowledge financial support from the DFG (Deutsche Forschungsgemeinschaft).

[1] a) T. Ishiguro, K. Yamaji, G. Saito, *Organic Superconductors*, Springer, Berlin **1990**; b) G. Saito, Y. Yoshida, *Bull. Chem. Soc. Jpn.* **2007**, *80*, 1–137; c) P. Batail, *Chem. Rev.* **2004**, *104*, 4887–4890; d) J.-I. Yamada, H. A. Nishikawa, K. Kikuchi, *Chem. Rev.* **2004**, *101*, 5057–5084; e) D. Jérome, *Chem. Rev.* **2004**, *104*, 5057–5084.

[2] See, for example: a) F. Schoenebeck, J. A. Murphy, S.-ze Zhou, Y. Uenoyama, Y. Miclo, T. Tuttle, *J. Am. Chem. Soc.* **2007**, *129*, 13368–13369; b) J. A. Murphy, S.-ze Zhou, D. W. Thomson, F. Schoenebeck, M. Mahesh, S. R. Park, T. Tuttle, L. E. A. Berlouis, *Angew. Chem.* **2007**, *119*, 5270–5275; *Angew. Chem. Int. Ed.* **2007**, *46*, 5178–5183; c) R. D. Richardson, T. Wirth, *Chem. Unserer Zeit* **2008**, *42*, 186–191; d) G. P. McGlacken, T. A. Khan, *Angew. Chem.* **2008**, *120*, 1843–1847; *Angew. Chem. Int. Ed.* **2008**, *47*, 1819–1823.

[3] a) J. S. Miller, K. S. Min, *Angew. Chem.* **2009**, *121*, 268–278; *Angew. Chem. Int. Ed.* **2009**, *48*, 262–272; b) M. D. Ward, J. A. McCleverty, *J. Chem. Soc., Dalton Trans.* **2002**, 275–288.

[4] A. Peters, E. Kaifer, H.-J. Himmel, *Eur. J. Org. Chem.* **2008**, 5907–5914.

[5] T. Soda, J. H. Hildebrand, *J. Phys. Chem.* **1967**, *71*, 4561–4563.

[6] Collaboration with Prof. J. Beck, University of Bonn.

[7] H. Ishida, S. Kashino, *Acta Crystallogr., Sect. C* **2001**, *57*, 476–479.

[8] E. K. Andersen, *Acta Crystallogr.* **1967**, *22*, 191–196.

[9] M. Reinmuth, U. Wild, E. Kaifer, M. Enders, H. Wadepohl, H.-J. Himmel, *Eur. J. Inorg. Chem.*, submitted for publication.

[10] We are currently studying the possibility of using this reaction for the fabrication of Cu nanoparticles by addition of some suitable size-limiting ligands. See, for example: a) T.-Y. Dong, H.-H. Wu, M.-C. Lin, *Langmuir* **2006**, *22*, 6754–6756; b) P. Kanninen, C. Johans, J. Merta, K. Kontturi, *J. Colloid Interface Sci.* **2008**, *318*, 88–95.

[11] D. Petrovic, L. M. R. Hill, P. G. Jones, W. B. Tolman, M. Tamm, *Dalton Trans.* **2008**, 887–894.

[12] P. C. A. Bruijnincx, M. Viciano-Chumillas, M. Lutz, A. L. Spek, J. Reedijk, G. van Koten, R. J. M. Klein Gebbink, *Chem. Eur. J.* **2008**, *14*, 5567–5576.

[13] O. Kahn, *Angew. Chem.* **1985**, *97*, 837–853; *Angew. Chem. Int. Ed. Engl.* **1985**, *24*, 834–850.

[14] E. Wasserman, L. C. Snyder, W. A. Yager, *J. Chem. Phys.* **1964**, *41*, 1763–1772.

[15] A. Peters, U. Wild, O. Hübner, E. Kaifer, J. Mautz, H.-J. Himmel, *Chem. Eur. J.* **2008**, *14*, 7813–7821.

[16] U. Wild, O. Hübner, A. Maronna, M. Enders, E. Kaifer, H. Wadepohl, H.-J. Himmel, *Eur. J. Inorg. Chem.* **2008**, 4440–4447.

[17] See, for example, the discussion in: N. Hebben, H.-J. Himmel, G. Eickerling, M. Reiher, V. Herz, M. Presnitz, W. Scherer, *Chem. Eur. J.* **2007**, *13*, 10078–10087.

[18] Additional XRD experiments, in which data were collected at higher angles, gave no improvement.

[19] L. S. Bartell, E. A. Roth, C. D. Hollowell, K. Kuchitsu, J. E. Young Jr, *J. Chem. Phys.* **1965**, *42*, 2683–2686.

[20] I. Krossing, A. Reisinger, *Angew. Chem.* **2003**, *115*, 5903–5906; *Angew. Chem. Int. Ed.* **2003**, *42*, 5725–5728.

[21] A. Peters, E. Kaifer, H.-J. Himmel, work in progress.

[22] J. H. Price, A. N. Williamson, R. F. Schramm, B. B. Wayland, *Inorg. Chem.* **1972**, *11*, 1280–1284.

[23] *DENZO-SMN, Data Processing Software*, Nonius, **1998**, ttp://www.nonius.com.

[24] a) G. M. Sheldrick, *SHELXS-97*, *Program for Crystal Structure Solution*, University of Göttingen, **1997**; http://shelx.uni-ac.gwdg.de/SHELX/index.html; b) G. M. Sheldrick, *SHELXL-97*, *Program for Crystal Structure Refinement*, University of Göttingen, **1997**; http://shelx.uni-ac.gwdg.de/SHELX/index.html.

[25] *International Tables for X-ray Crystallography*, Kynoch Press, Birmingham, UK, **1974**, vol. 4.

[26] L. Zsolnai, G. Huttner, *XPMA*, University of Heidelberg, **1994**; http://www.uni-heidelberg.de/institute/fak12/AC/huttner/software/software.html.

Received: May 4, 2009
Published Online: July 24, 2009

